SATBAYEV UNIVERSITY

Engineering Journal of Satbayev University

Volume 148 (2026), Issue 5, 27-34

https://doi.org/10.51301/ejsu.2026.i5.03

Microstructure, internal friction and impact-induced acoustic response of newly developed alloyed steels

R.Zh. Abuova*, G.A. Burshukova, Ye.S. Merkibayev

International Educational Corporation, Almaty, Kazakhstan

**Corresponding author: ryskena@mail.ru*

Abstract. This study evaluates the relationships among mechanical energy dissipation, elastic stiffness, electrical resistivity, microstructural heterogeneity and impact-induced sound radiation in three newly developed alloyed steels (XSM-1, XSM-2 and XSM-3). Standard carbon steels St.10, St.20 and St.45 were used as reference materials. Plate specimens (50×50×5 mm) underwent steel-ball impact testing, with transient oscillograms captured in a 2 ms observation window; torsional oscillation measurements, sound-level measurements and metallographic observations provided complementary evidence. XSM-1 exhibited the greatest tabulated internal friction (21.22×10^{-4}) and the lowest A-weighted sound level (72 dBA), compared with 9.11-10.565×10^{-4} and 84-89 dBA for the reference steels. XSM-2 reached 77 dBA and XSM-3 87 dBA, despite both having relatively high internal friction. The descriptive Pearson association between internal friction and sound level across the six materials was approximately −0.70, whereas elastic modulus values did not show a clear monotonic pattern. Micrographs available for XSM-3 indicate structural heterogeneity but do not provide definitive phase identification. The results suggest that intrinsic material damping is important but insufficient on its own to predict impact noise; modal response, microstructure and testing configuration should be considered jointly. The study identifies XSM-1 as the leading candidate within this limited comparative dataset and specifies the measurements needed for independent validation.

Keywords: *alloyed steel, internal friction, impact noise, vibration damping, microstructure, elastic modulus, electrical resistivity, acoustic emission.*

Received: 12 October 2026
Received in revised form: 11 July 2026
Accepted: 16 October 2026
Available online: 31 October 2026

1. Introduction

Reduction of vibration and the accompanying noise remains an important materials-engineering problem in machines and mechanisms. Impact and cyclic interactions between metallic components generate elastic waves that are partly radiated as airborne sound and partly dissipated within the material. Increasing the intrinsic damping of structural metals is therefore attractive because it acts at the source of vibration rather than relying exclusively on external isolators or polymeric damping layers.

High-damping metallic systems include Mn-Cu, Fe-Cr, Ni-Ti, Mg-based and Fe-Mn alloys. Recent work has renewed interest in Fe-Mn and Fe-Mn-Cr systems because their damping response can be controlled through martensitic transformations, stacking faults, phase boundaries, grain structure and heat treatment. Yan et al. showed that rapid solidification of Fe-17Mn promotes ε-martensite and increases damping capacity [1]. He et al. demonstrated that the optimum Mn content of cast Fe-Mn binary alloys differs from deformation-processed alloys and is close to 19 wt.% in the cast state [2]. More recent alloy-design strategies combine grain refinement with ε-martensite introduction to obtain a better balance between strength and damping [3]. Comparative studies have also examined differences in microstructure, damping capacity, and mechanical properties between cast and deformation-processed Fe17Mn alloys [4]. Fe–Mn–Cr composite alloys have been investigated as a means of combining damping capacity, mechanical strength, and corrosion resistance [5].

Other metallic damping systems also demonstrate strong relationships between microstructure and energy dissipation. Orientation-dependent damping behavior has been investigated in Mn–Cu shape memory alloys [6], while the formation of nanodomains in Ni–Ti alloys has been associated with enhanced damping capacity [7]. The influence of long-period stacking-ordered phases on damping behavior has also been examined in magnesium alloys [8]. In FeMnCrCo high-entropy alloys, stacking fault energy and lattice distortion have been investigated as factors controlling damping mechanisms [9]. Furthermore, the effects of manganese content on microstructural evolution and mechanical properties have been studied in cast Fe–Mn damping alloys [10].

These studies demonstrate that damping is a structure-sensitive property. Grain boundaries, dislocations, stacking faults, phase interfaces and local chemical heterogeneity provide mechanisms for irreversible or hysteretic energy

© 2026. R.Zh. Abuova, G.A. Burshukova, Ye.S. Merkibayev
ryskena@mail.ru; gulziya.burshukova@gmail.com; erik_me@mail.ru
Engineering Journal of Satbayev University. eISSN 2959-2348. Published by Satbayev University
This is an Open Access article distributed under the terms of the Creative Commons Attribution License (http://creativecommons.org/licenses/by/4.0/), which permits unrestricted reuse, distribution, and reproduction in any medium, provided the original work is properly cited.

loss. At the same time, the acoustic response of a real plate under impact is governed not only by intrinsic damping but also by elastic stiffness, geometry, excitation amplitude and the distribution of structural heterogeneities. Consequently, a high value of one material parameter does not necessarily guarantee the lowest radiated sound level.

Machine-generated noise is not solely an acoustic-design issue; it is also a structural-materials problem. Metallic housings, frames, supports and rotating components can transmit transient stresses through connected structures, which then radiate sound into surrounding air. An impact creates multiple resonant modes simultaneously, and their decay depends on the interaction between the input force, geometry, boundary conditions, mass distribution and constitutive response. In many conventional engineering designs, noise mitigation is implemented after a component has been manufactured through added dampers, isolators, enclosures or changes to assembly interfaces. Material-level damping can offer a complementary approach, potentially reducing the vibratory energy available for subsequent transmission. Unlike an attached polymer layer, intrinsic metal damping is embedded throughout the load-bearing material, although the overall benefit still requires evaluation at component and system level.

A useful distinction must be drawn between the mechanical loss of vibrational energy and the sound pressure measured at a microphone. Internal friction describes irreversible or delayed processes within a cyclically strained solid. Acoustic emission, in the broad sense used here for impact-generated radiated sound, results from surface velocity fields coupled to the surrounding air. The two quantities are related through the vibration problem but are not interchangeable. Even if a material loses more mechanical energy per oscillation cycle, the sound level can remain relatively high if the impact couples efficiently to a radiating mode, the mode shape changes, or the excitation spectrum shifts toward more efficiently radiating frequencies. This distinction motivates the combined measurement strategy used in the present work.

High-damping materials are often classified by their dominant loss mechanisms. Dislocation-mediated damping can arise from the reversible bowing of pinned dislocation segments and their nonlinear depinning under higher amplitudes. Ferromagnetic alloys can lose energy through magnetic-domain-wall motion. Twinning and martensitic transformations generate mobile phase and twin boundaries, while multiphase alloys can exhibit interfacial hysteresis and localized deformation. These broad categories provide mechanistic hypotheses, not direct proof that any one pathway dominates the XSM steels. A metallographic image alone cannot determine the density or mobility of such defects, and conventional optical contrast cannot reliably identify a crystallographic phase without corroborating diffraction or compositional data.

Recent research has demonstrated the practical importance of processing history in Fe–Mn damping alloys. Yan and coworkers reported enhanced ε-martensite formation and damping after rapid solidification of Fe–17Mn [1]. He and colleagues found that the optimum manganese content for cast Fe–Mn binary damping alloys differs from that of deformation-processed counterparts, with an optimum near 19 wt.% under their conditions [2]. A later strength–damping study combined grain refinement with the introduction of ε-martensite, demonstrating that strengthening strategies can help or hinder damping depending on the retained mobile interfaces [3]. Research published in 2026 further illustrates how deformation sequencing [11] and additive manufacturing followed by annealing [12, 13] can strongly alter the microstructure–damping relationship. These studies establish an active contemporary context for investigations of structure-sensitive damping, but their detailed phase mechanisms should not be assumed to apply directly to the present steels without composition and phase analysis.

A-weighted sound levels are commonly used in occupational noise exposure assessment [14]. Because acoustic noise commonly spans a broad frequency interval, a single A-weighted level provides an informative but incomplete description. A weighting reflects a standardized frequency sensitivity and compresses spectral information into one number. Two specimens with the same dBA value may have different octave-band spectra and very different vibration signatures. Conversely, a measurable change in dBA does not by itself reveal how much mechanical energy was dissipated internally. Thus, measurements of sound, resonant decay, elastic properties and metallography are best interpreted as complementary observations instead of interchangeable proxies. This is especially relevant when comparative tests are conducted on relatively small plate specimens rather than fully engineered machine parts.

The specific research question is whether the three developed XSM steels exhibit improved impact-acoustic behavior relative to conventional carbon steels and whether that response can be explained by a single measured bulk parameter. The working hypothesis is that enhanced internal friction will generally favor lower sound radiation, but that the observed acoustic outcome will also reflect structural and dynamic factors. A secondary objective is to identify limitations of the existing experimental record and define a defensible verification program for subsequent alloy optimization.

2. Materials and methods

2.1. Materials and experimental scope

The investigated set consisted of three standard carbon steels (St.10, St.20 and St.45) and three newly developed alloyed steels designated XSM-1, XSM-2 and XSM-3. The experimental draft reports melting and subsequent heat treatment of the developed alloys. Plate specimens with dimensions 50×50×5 mm was used for stiffness and vibroacoustic measurements. The microstructural observations presented below correspond to XSM-3 in the polished unetched condition and after metallographic etching. The available records do not give a complete, internally consistent spectrometric composition for each XSM grade; therefore, no elemental concentrations are inferred in this analysis.

The experiments were evaluated as a six-material comparative series rather than as a factorial design. The reference materials were St.10, St.20 and St.45; the newly developed materials were XSM-1, XSM-2 and XSM-3. In the source documentation, certain earlier labels for experimental iron–carbon specimens appear alongside the final XSM nomenclature. Because an explicit specimen-by-specimen equivalence is unavailable, the quantitative comparative tables use only the consistent XSM designations. Results for a duralumin specimen and unfilled damping-decrement fields are discussed as contextual observations where appropriate, but they are excluded from the principal six-steel dataset.

A reproducible comparison of vibration-damping steels would ideally specify chemical composition, melting atmosphere, casting geometry, homogenization temperature, subsequent heat treatment, machining orientation and surface finish. These factors affect defects, residual stress, segregation and phase stability. The supplied manuscripts mention melting and heat treatment, but not all relevant parameters are documented in a way that supports independent reconstruction. Consequently, this paper reports the observed relationships in the available specimens; it does not claim an optimized processing route or an unambiguous causal effect of a particular alloying element.

2.2. Measurement of elasticity and internal friction

The shear modulus (G) was determined by a torsional-oscillation method based on the natural oscillation period of the specimen. Young's modulus (E) was calculated from the shear modulus using the Poisson ratio adopted in the experimental procedure. Internal friction was used as the principal integral characteristic of mechanical-energy dissipation. The original experimental setup for measuring shear modulus and internal friction under free and forced oscillations is shown in Figure 1.

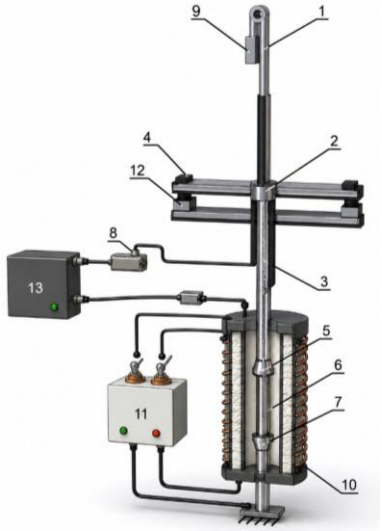


Figure 1. Apparatus used in the source experiments for torsional-oscillation modulus and internal-friction measurements: 1 – nylon thread; 2 – frame; 3 – rod; 4 – electromagnets; 5, 7 – collet clamps; 6 – specimen; 8 – rheostat; 9 – weight; 10 – furnace; 11 – temperature controller; 12 – optical system; 13 – signal generator

For approximately isotropic linear elastic behavior, Young's modulus E and shear modulus (G) are related by $E = 2G(1+\nu)$, where ν denotes Poisson's ratio. This relation expresses an assumed continuum model and should not be used to infer phase-specific stiffness. The original measurement procedure derives (G) from the period of torsional oscillation and geometric or calibration constants of the apparatus. Because the complete calibration parameters are not available in the supplied material, the tabulated values are retained as reported rather than recalculated from the oscillation periods.

Internal friction is commonly expressed in dimensionless form as Q^{-1}, which for weakly damped linear oscillations can be related to the logarithmic decrement (δ) approximately by $Q^{-1} \approx \delta/\pi$. Such equivalence depends on measurement regime and convention; more generally, the mechanical loss factor is defined as energy dissipated per cycle divided by 2π times the maximum stored energy. The numerical internal-friction values in this manuscript are reproduced from the experimental tables without assuming that the missing logarithmic-decrement observations can be recovered. Their units and scale are presented exactly as tabulated, 10^{-4}, to avoid confusing them with values reported on other experimental scales.

The measurement apparatus, depicted in Figure 1, comprises a supported specimen, a mechanical excitation arrangement and a detection system for free and forced oscillations. Oscillatory testing is useful for distinguishing stored elastic energy from internal losses, but both quantities can depend on temperature, frequency, strain amplitude and specimen condition. Accordingly, the reported internal-friction values represent the particular experimental measurement state and should not automatically be treated as frequency-independent material constants over all practical service conditions.

2.3. Impact-acoustic measurements

Acoustic and damping characteristics of the plate specimens were evaluated under impact excitation by steel-ball impact. Decay oscillograms were recorded using a PCS-500 oscilloscope over a 2 ms time window. The recorded signal characterizes the transient response after impact and allows qualitative comparison of the decay rate. Sound level was expressed in dBA. The source manuscript also reports sound-pressure measurements in octave bands from 125 to 8000 Hz. Only the integral sound-level values that are consistently tabulated for all six materials are used in the comparative analysis below.

In an impact-response measurement, the force–time history of the striking body determines the spectrum of injected energy. The ball material, diameter, mass, release height or velocity and contact conditions can therefore influence the resulting signal, independently of the tested metal. The supplied study identifies a steel-ball impact method but does not give a complete and consistently associated set of these impact parameters for each specimen. Results are consequently interpreted as comparative observations under the reported laboratory procedure, rather than as an absolute prediction of field noise.

The 2 ms oscilloscope record is particularly sensitive to early transient behavior. It can reveal the initial distribution of peaks and the qualitative rate at which an oscillatory envelope decreases. However, without numerical trace exports, identical vertical gains, calibration and a specified envelope-fitting method, precise logarithmic decrement, modal damping ratio and frequency-selective loss cannot be reconstructed reliably. The A-weighted acoustic measurements and the oscilloscope traces are therefore considered separately: the former provide the principal cross-material numerical ranking; the latter provide visual corroboration only. The underlying experimental notes additionally refer to octave-band assessments between 125 and 8000 Hz, but complete numerical band-by-band measurements were not available for all six materials.

2.4. Metallography and data-analysis strategy

Metallographic examination was carried out on polished surfaces before etching and after etching. The unetched surface was used to reveal inclusions, pores and segregation-related defects, whereas etching was used to reveal grain and phase morphology. For the six-material dataset, Pearson correlation coefficients were calculated as descriptive indicators only; because $n = 6$, they are not treated as proof of a universal functional relationship.

Metallographic images before etching emphasize surface-visible inclusions and other heterogeneities, while etched images make grain-scale morphology and boundary contrasts easier to inspect. However, etching contrast is sensitive to reagent, exposure and preparation history. A bright feature cannot be assigned uniquely to ferrite, a carbide or a second phase without orthogonal evidence. Here, qualitative metallography is used to formulate hypotheses about heterogeneous elastic-wave propagation, not to quantify phase fractions, grain-size distributions or defect densities.

All comparisons are descriptive. Pearson correlations were evaluated across the six reported material-grade observations, with each grade contributing one tabulated row. With this small sample, between-grade variation may reflect many coupled material differences, and statistical significance would be unstable. No confidence interval for a mean, standard deviation, hypothesis-test p value or repeatability estimate is reported because underlying replicate measurements are not supplied. Likewise, differences in decibel values are correctly treated as differences on a logarithmic level scale, rather than as direct arithmetic differences in acoustic power or subjective loudness.

3. Results and discussion

3.1. Comparison of sound radiation and internal friction

The developed steels show a substantially different dissipative response from the reference grades (Table 1). XSM-1 has the highest internal friction, 21.22×10^{-4}, and the lowest measured sound level, 72 dBA. XSM-2 combines 20.16×10^{-4} internal friction with 77 dBA. XSM-3 retains a relatively high internal-friction value of 19.24×10^{-4} but its sound level rises to 87 dBA. In comparison, St.45, St.20 and St.10 show internal-friction values of $9.11\text{-}10.565\times10^{-4}$ and sound levels of 84-89 dBA. Thus, XSM-1 reduces the integral sound level by 17 dBA relative to St.45 and by 12 dBA relative to St.20, while its internal friction is approximately 2.3 times that of St.45.

Table 1. Reported internal friction, electrical resistivity and A-weighted sound level.

Material	Internal friction, $\times10^{-4}$	Electrical resistivity, $\times10^{-4}\Omega\cdot$m	Sound level, dBA
St.45	9.11	12.24	89
St.20	9.18	13.16	85
St.10	10.565	12.96	84
XSM-1	21.22	14.25	72
XSM-2	20.16	14.28	77
XSM-3	19.24	14.26	87

For the complete six-material set, the Pearson coefficient between internal friction and sound level is $r \approx -0.70$. This moderate inverse association is physically consistent with the expectation that greater internal dissipation can reduce the energy available for acoustic radiation. Nevertheless, XSM-3 demonstrates that internal friction alone does not uniquely determine the emitted sound: despite its high internal friction, its sound level is close to that of the standard steels. The result points to additional effects of phase morphology, elastic response, defect distribution and impact-coupled vibration modes.

Electrical resistivity is higher for XSM-1-XSM-3 ($14.25\text{-}14.28\times10^{-6}\,\Omega\cdot$m) than for the standard steels ($12.24\text{-}13.16\times10^{-6}\,\Omega\cdot$m). The descriptive correlation with sound level is negative ($r \approx -0.66$), but the three XSM alloys have almost identical resistivity and markedly different sound levels. Resistivity should therefore be regarded as a structure-sensitive complementary indicator rather than a direct predictor of acoustic damping.

The comparison reveals two distinct outcomes. First, all three newly developed steels have substantially greater tabulated internal friction than the conventional grades. The smallest value among the developed materials (XSM-3, 19.24×10^{-4}) still exceeds the largest reported reference value (St.10, 10.565×10^{-4}). This separation suggests that the alloy development procedure changed the mechanisms responsible for mechanical loss, although the dataset does not specify which microstructural contribution was decisive. Second, the improvement in sound level is not uniform across all three candidate materials. The high internal friction of XSM-3 does not translate into a comparably low A-weighted level, making that alloy an important counterexample to a simple single-parameter selection rule.

Relative to St.45, the XSM-1 measured sound-level difference is 17 dB, while the corresponding difference relative to St.10 is 12 dB. These comparisons are meaningful as logarithmic sound-level differences under the same stated measurement procedure. If one assumed identical A-weighting, measurement geometry and acoustic reference conventions, a 17 dB difference corresponds to a factor of approximately 50 in the associated mean-square acoustic pressure quantity. That calculation should not be interpreted as a direct measurement of mechanical energy dissipated, radiated sound power or perceived loudness. Those outcomes require separate calibration and physical interpretation.

The reported resistivity values for the new steels are tightly clustered: 14.25, 14.28 and $14.26\times10^{-6}\,\Omega\cdot$m for XSM-1, XSM-2 and XSM-3, respectively. By contrast, their sound levels span from 72 to 87 dBA. This near-equality of one electrical measurement alongside a large separation in acoustic response is particularly informative. Resistivity can be affected by solute atoms, phase fractions, vacancies, dislocations and other scattering centers for conducting electrons, but the present measurements cannot distinguish among those causes. In this dataset, resistivity provides evidence of differences between the developed and reference classes but lacks resolution to predict the ranking within the new class.

3.2. Elastic properties versus impact sound level

The shear modulus varies within a relatively narrow interval of $8.054\text{-}8.49\times10^{10}$ Pa, while Young's modulus ranges from 19.81 to 20.89×10^{10} Pa. These changes are small compared with the 17 dBA span in measured sound level. XSM-1, which has the lowest sound level, does not have an extreme value of either elastic modulus. The descriptive correlations are $r \approx 0.07$ for shear modulus and $r \approx -0.18$ for Young's modulus, confirming the absence of a simple monotonic relationship in this dataset (Table 2).

This observation is important for interpretation. Elastic moduli determine stiffness and influence natural frequencies and wave velocities, but acoustic attenuation is governed by energy-loss mechanisms. Consequently, the sound level under impact should be interpreted through the combined effects of stiffness, damping, microstructure and excitation conditions rather than through Young's modulus or shear modulus alone.

Table 2. Reported oscillation periods, elastic moduli and sound levels

Material	Oscillation period (*T*), s	T^2, s^2	Shear modulus G, $\times 10^{10}$ Pa	Young's modulus (*E*), $\times 10^{10}$ Pa	Sound level, dBA
St.45	0.1836	0.0337	8.175	20.11	89
St.20	0.1822	0.0332	8.054	19.81	85
St.10	0.1811	0.0333	8.080	19.88	84
XSM-1	0.1845	0.0340	8.248	20.29	72
XSM-2	0.1862	0.0347	8.148	20.71	77
XSM-3	0.1877	0.0350	8.490	20.89	87

Elastic moduli influence the dynamic stiffness of a plate and, in combination with density and geometry, its characteristic mode frequencies. A stiffness increase can shift resonance peaks away from or toward the dominant frequencies in an impact excitation or a microphone weighting curve. It may also alter the contact duration and initial velocity response of the plate. Consequently, a monotonic association between one modulus and integrated sound level is not expected in general. The present data illustrate this point: XSM-3 has the highest reported *G* and *E* and a relatively high sound level, but XSM-1 has neither the lowest nor highest modulus while giving the lowest sound level.

An additional reproducibility check is warranted for the reported dynamic parameters. The elastic relationship between *E*, *G* and *ν* is straightforward, yet the tabulated *E* and *G* pairs are not all compatible with a single fixed Poisson ratio if taken literally. This may arise from independent determinations, rounding, transcription or different assumed conventions. Because the original calibration and raw measurements are unavailable, the data have not been silently harmonized. Future experiments should provide the exact relation, ν values and uncertainty for each grade. The periods and their squares should also be recalculated from raw timing records before submission, given that some printed squared-period values are rounded and do not exactly match the displayed periods.

3.3. Transient acoustic signals

The oscillograms show distinct transient-decay patterns (Figure 2). The standard St.10 signal retains a comparatively extended oscillatory envelope, whereas the developed steels exhibit modified decay behavior. The source draft describes faster reduction of the sound impulse for the damping compositions and a lower integral sound level for XSM-1.

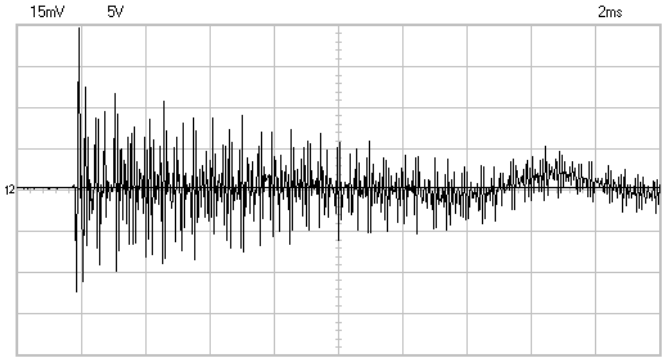


Figure 2. Example transient oscillogram reproduced from the source material; interpretation is qualitative because raw voltage–time points and calibration are unavailable

Because the original manuscript contains blank placeholders for logarithmic decrement, relative scattering and Q^{-1} values derived from these specific traces, no missing numerical values are reconstructed in the present version. The oscillograms are therefore used as qualitative support, while the quantitative comparison relies on the tabulated internal-friction and sound-level data.

Several additional observations are recorded in the Russian-language experimental report. The reference St.10 specimen was described as exhibiting an initially high and gradually declining sound impulse, while selected developed samples showed altered signal envelopes and a more rapid drop in measured peaks. The same account mentions a duralumin D16 comparison exhibiting multiple peaks over the record. However, the narrative uses earlier experimental labels in places where the figure captions use XSM designations. Rather than assigning these observations to uncertain material identities, the present analysis preserves only the qualitative statement that transient decay differed among the tested specimens.

To convert such information into a rigorous amplitude-dependent damping result, each voltage trace should be acquired under calibrated and identical impact conditions. The logarithm of the oscillation envelope could then be fitted against time for a selected mode and reported with a goodness-of-fit measure. Measurements would need to be repeated at several impact energies or strain amplitudes to test the nonlinear contribution of dislocation unpinning, interface mobility or other amplitude-sensitive processes. Since this validation was not present in the available records, the manuscript does not claim a numerical amplitude-dependence exponent or an experimentally established threshold strain.

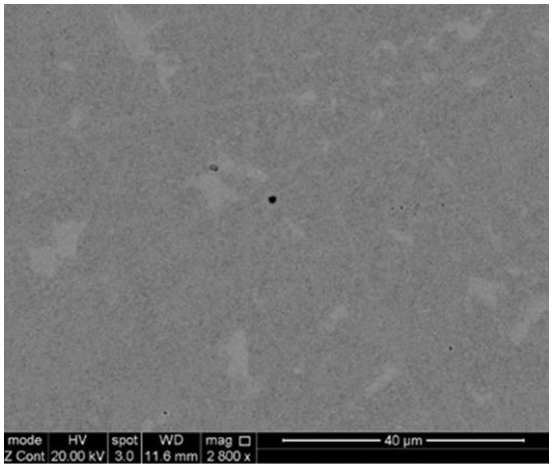
3.4. Microstructural evidence

A steel microstructure is an elastically heterogeneous polycrystalline medium. Neighboring grains differ in crystallographic orientation and local elastic response; phase boundaries, grain boundaries, inclusions, pores, segregation zones and lattice defects introduce additional discontinuities. When an elastic wave propagates through such a medium, part of its energy is redistributed by scattering and part is dissipated by irreversible defect and interface processes. This provides a physical basis for linking metallographic state with impact-acoustic behavior, while also explaining why a single bulk elastic modulus cannot fully describe damping.

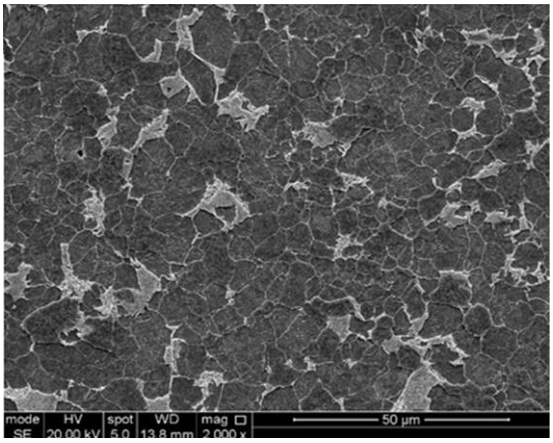
Before etching, the XSM-3 surface contains dark local features interpreted in the source manuscript as non-metallic inclusions and segregation cavities (Figure 3). After etching, the structural relief is much more pronounced and a ferrite-pearlite morphology is reported (Figure 4). Such heterogeneity creates multiple characteristic length scales for interaction with elastic waves.

Grain and phase boundaries can contribute to scattering, while mobile defects and interfaces can contribute to internal friction. The damping response is therefore expected to depend on the density, morphology and mobility of these structural elements rather than on grain size alone.

The metallographic information is limited principally to XSM-3. It therefore cannot by itself establish why XSM-1 has the best acoustic performance. In particular, no parallel quantitative microstructure study of XSM-1 and XSM-2 is documented in the supplied material. The visible XSM-3 heterogeneity nevertheless supports the more general proposition that the developed material is not a perfectly homogeneous continuum.

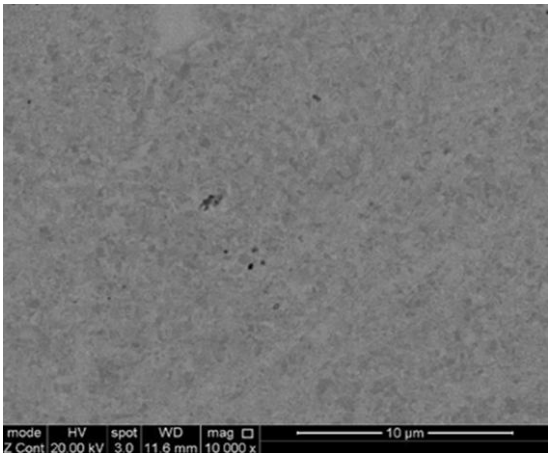


(a)

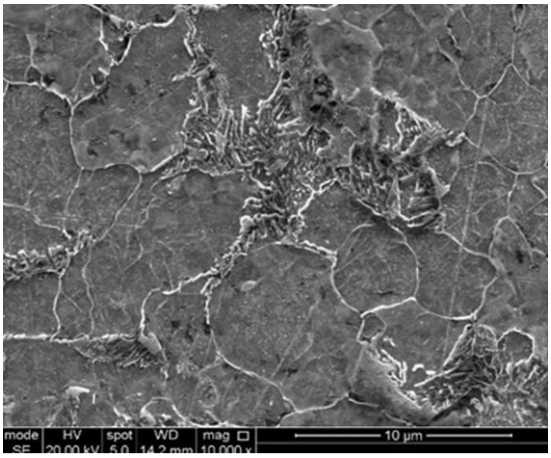


(b)

Figure 3. Representative XSM-3 micrograph from the original polished/unetched observations; contrast is not sufficient for definitive constituent identification



(a)



(b)

Figure 4. Representative XSM-3 micrograph after etching, showing heterogeneous morphology and visible boundaries

Differences in phase and grain morphology could create spatial fluctuations in impedance and localized deformation. Such heterogeneity may modify the pathways by which elastic waves are reflected, transmitted or irreversibly damped.

Scattering and dissipation must be distinguished conceptually. Elastic scattering redistributes wave energy among directions, frequencies or modes; it does not necessarily convert vibrational energy to heat. Dissipation requires an irreversible or delayed response, such as defect motion, interface hysteresis or thermoelastic relaxation. An optical micrograph cannot measure the partition between these processes. To establish an actual mechanism, supplementary scanning electron microscopy, electron backscatter diffraction, X-ray diffraction, chemical microanalysis and frequency- and amplitude-resolved mechanical spectroscopy would be needed.

Among the investigated materials, XSM-1 provides the most favorable combination of low sound level and high internal friction. XSM-2 is also clearly superior to the reference steels by sound level, whereas XSM-3 illustrates that high internal friction does not automatically translate into low acoustic emission. For engineering selection, this means that screening of damping steels should combine at least three levels of characterization: intrinsic dissipation (internal friction or loss factor), structural characterization (grain/phase morphology and defects), and component-relevant acoustic or vibration testing under representative excitation.

The current dataset is sufficient to rank the investigated steels under the applied test conditions, but it does not yet establish a universal predictive model. Future work should report verified chemical compositions for all XSM grades, repeated measurements with uncertainty estimates, quantitative grain-size/phase-fraction analysis, and frequency-resolved damping. Such additions would enable statistically supported structure-property relationships and strengthen transfer of the results to real machine components.

Its measured 72 dBA result offers a motivation to investigate machine brackets, enclosures, supports, gear-related components or other dynamically excited parts. However, successful transfer from a small laboratory plate to a real assembly would require compatible heat treatment, fatigue performance and manufacturability. Most importantly, the material should be evaluated in the intended component geometry, where boundary conditions and modal radiation are likely to differ substantially from those of the screening specimens.

4. Conclusions

The newly developed XSM steels exhibit higher internal friction than St.10, St.20 and St.45. XSM-1 reached 21.22×10^{-4} and showed the lowest sound level, 72 dBA.

Relative to St.45, XSM-1 reduced the measured integral sound level by 17 dBA. XSM-2 showed 77 dBA, while XSM-3 showed 87 dBA, indicating that the developed compositions do not behave identically under impact excitation.

Internal friction shows a moderate inverse association with sound level across the six materials, but the XSM-3 result confirms that damping cannot be predicted from internal friction alone.

No simple monotonic dependence of sound level on shear modulus or Young's modulus was observed. Elastic stiffness should therefore be considered together with dissipative and microstructural characteristics.

Metallographic observations of XSM-3 before and after etching demonstrate structural heterogeneity and reveal grain/phase morphology that can participate in scattering and internal-friction mechanisms. The combined acoustic-damping-microstructural approach is recommended for selecting steels for dynamically and impact-loaded machine components.

The key practical recommendation is to prioritize XSM-1 for repeatable, frequency-resolved testing while using XSM-3 as a mechanistically informative contrast. Verification of chemical compositions, structural phases, calibration records and replicate statistics is essential before submitting claims of an optimized alloy or deploying these steels in safety-critical machine components.

Author contributions

Conceptualization: RZA, GAB; Data curation: RZA; Formal analysis: RZA; Funding acquisition: RZA, GAB; Investigation: RZA; Methodology: GAB, RZA; Project administration: RZA, GAB; Resources: RZA, YSM; Software: YSM; Supervision: RZA, YSM; Validation: RZA, YSM; Visualization: RZA; Writing – original draft: GAB, RZA; Writing – review & editing: RZA, YSM. All authors have read and agreed to the published version of the manuscript.

Funding

This research was funded by Science Committee of the Ministry of Science and Higher Education of the Republic of Kazakhstan, grant number AP27511849 «Development of alloy steels with dissipative properties and their surface modification by deposition of nanostructured wear-resistant coatings for critical components in mechanical engineering».

Acknowledgements

The authors gratefully acknowledge the contributions of the editor and reviewers, whose thoughtful observations, constructive criticism, and detailed recommendations were instrumental in improving the manuscript. Their careful consideration of the research methodology, presentation of experimental findings, and interpretation of the results provided valuable guidance during the revision process. The authors particularly appreciate the reviewers' efforts to identify areas requiring further clarification and to suggest improvements that enhanced overall quality of the study.

Conflicts of interests

The authors declare no conflict of interest.

Data availability statement

The original contributions presented in this study are included in the article. Further inquiries can be directed to the corresponding author.

References

[1] Yan, N., Geng, D., & Wei, B. (2022). Damping performance and martensitic transformation of rapidly solidified Fe-17%Mn alloy. *Journal of Materials Science & Technology*, *117*, 1-7. https://doi.org/10.1016/j.jmst.2021.10.042

[2] He, W., Qiu, H., Zeng, X., Wang, Y., Luo, Y., Fu, Y., Peng, H., & Wen, Y. (2024). Damping capacity in cast FeMn binary alloys. *Journal of Alloys and Compounds*, *1008*, 176513. https://doi.org/10.1016/j.jallcom.2024.176513

[3] Xie, X.G., Chen, J., & Cao, G.M. (2025). 800 MPa Fe–Mn alloy with expected damping capacity by coupling grain refinement and ε-martensite introduction. *Journal of Iron and Steel Research International*, *32*, 2504-2511. https://doi.org/10.1007/s42243-024-01392-2

[4] He, W., Wang, Y., Yuan, Y., Luo, Y., Peng, H., & Wen, Y. (2024). Comparison of microstructure, damping capacity, and mechanical properties of cast and deformation processed Fe17Mn alloys. *Materials Today Communications*, *39*, 108972. https://doi.org/10.1016/j.mtcomm.2024.108972

[5] He, W., Yuan, Y., Yan, J., Huang, Y., Peng, H., & Wen, Y. (2024). High-strength corrosion-resistant FeMnCr-based composite damping alloys fabricated by vacuum annealing. *Journal of Alloys and Compounds*, *977*, 173345. https://doi.org/10.1016/j.jallcom.2023.173345

[6] Zuo, S., Xiao, F., & Fukuda, T. (2019). Orientation dependence of damping behavior in a Mn–Cu shape memory alloy. *Scripta Materialia*, *170*, 95-98. https://doi.org/10.1016/j.scriptamat.2019.05.042

[7] Song, Y., Jin, M., Han, X., Wang, X., Chen, P., & Jin, X. (2021). Microstructural origin of ultrahigh damping capacity in Ni50.8Ti49.2 alloy containing nanodomains induced by insufficient annealing and low-temperature aging. *Acta Materialia*, *205*, 116541. https://doi.org/10.1016/j.actamat.2020.116541

[8] Zhao, C., Wang, F., Li, J., Zeng, J., Dong, S., Wang, F., Jin, L., & Dong, J. (2024). Probing the varying ranges of damping capacity of magnesium alloys containing long-period stacking ordered phases. *Scripta Materialia*, *240*, 115845. https://doi.org/10.1016/j.scriptamat.2023.115845

[9] Zhang, Q., Xiong, W., Zhu, X., Chen, Z., Cui, M., Tian, Q., Zhu, X., & Xu, Y. (2025). Coordinating the damping mechanisms of FeMnCrCo high-entropy alloys by regulating the stacking fault energy and lattice distortion. *Materials Science and Engineering: A*, *948*, 149334. https://doi.org/10.1016/j.msea.2025.149334

[10] He, W., Wang, F., Lu, J., Wang, Y., Fu, Y., Peng, H., & Wen, Y. (2025). Dependence of microstructure evolution and mechanical properties on Mn contents in cast Fe(15–21)Mn damping alloys. *Materials Characterization*, *228*, 115417. https://doi.org/10.1016/j.matchar.2025.115417

[11] Yuan, X., Li, X., & Chen, L. (2026). Timing and level of cold deformation influence on microstructural evolution and damping properties of a Fe-17Mn quenched steel. *Materials Letters*, *403*, 139429. https://doi.org/10.1016/j.matlet.2025.139429

[12] Xiao, Y., Yan, J., Li, N., Li, R., Wang, L., Wu, Q., Peng, H., Wen, Y., Sang, L., Zhang, Y., & Zhou, Y. (2026). Mechanical and damping properties of selective laser-melted Fe–Mn damping alloy. *Advanced Engineering Materials*, *28*(6), e202502737. https://doi.org/10.1002/adem.202502737

[13] Ma, C., Huang, K., Wang, C., Liu, C., Liu, Z., & Chen, Z. (2025). Research progress on additive manufacturing of Mn–Cu damping alloys. *Journal of Alloys and Compounds*, *1034*, 181329. https://doi.org/10.1016/j.jallcom.2025.181329

[14] National Institute for Occupational Safety and Health. (1998). Criteria for a recommended standard: Occupational noise exposure (Revised criteria 1998) (DHHS (NIOSH) Publication No. 98-126). https://www.cdc.gov/niosh/docs/98-126/

Микроқұрылым, ішкі үйкеліс және жаңа легирленген болаттарға әсер ету кезіндегі акустикалық жауап

Р.Ж. Абуова*, Г.А. Буршукова, Е.С. Меркибаев
Халықаралық білім беру корпорациясы, Алматы, Қазақстан
**Корреспонденция үшін автор: ryskena@mail.ru*

Аңдатпа. Бұл зерттеу механикалық энергияның диссипациясы, серпімді қаттылық, электр кедергісі, микроқұрылымдық гетерогенділік және легирленген Болаттың үш жаңа түрі (XSM-1, XSM-2 және XSM-3) үшін соққы әсерінің дыбыстық сәулеленуі арасындағы байланысты бағалайды. Анықтамалық материалдар ретінде 10-бап, 20-бап және 45-бап маркалы стандартты көміртекті болаттар пайдаланылды. Пластина тәрізді үлгілер (50×50×5 мм) болат шардың соққысына сыналды; 2 мс бақылау терезесінде өтпелі осциллограммалар тіркелген. Қосымша мәліметтер бұралу тербелісі мен дыбыс деңгейін өлшеу кезінде, сондай-ақ металлографиялық зерттеулер жүргізу кезінде алынды. XSM-1 болаты ең үлкен ішкі үйкелісті (21.22×10^{-4}) және A шкаласы бойынша ең төменгі дыбыс деңгейін (72 дБА) көрсетті, ал анықтамалық болаттар үшін бұл көрсеткіштер сәйкесінше $9.11\text{-}10.565\times10^{-4}$ және 84-89 дБА болды. XSM-2 және XSM-3 болаттары үшін дыбыс деңгейлері екі жағдайда да салыстырмалы түрде жоғары ішкі үйкеліске қарамастан 77 дБА және 87 дБА құрады. Зерттелген барлық алты материал үшін Пирсонның ішкі үйкеліс пен дыбыс деңгейі арасындағы корреляция коэффициенті шамамен -0.70 болды, ал серпімділік Модулінің мәндері айқын монотонды қатынасты таппады. XSM-3 болатының микрографтары құрылымдық гетерогенділікті көрсетеді, бірақ фазалық құрамды біржақты анықтауға мүмкіндік бермейді. Нәтижелер материалдың ішкі демпфері маңызды рөл атқаратынын көрсетеді, бірақ оның өзі соққы шуын болжау үшін жеткіліксіз; факторлардың жиынтығын ескеру қажет: модальды жауап, микроқұрылым және сынақ шарттары. Осы салыстырмалы зерттеу аясында XSM-1 болаты ең перспективалы нұсқа ретінде анықталды; алынған нәтижелерді тәуелсіз тексеру үшін қажетті өлшемдер тізімі де анықталды.

Негізгі сөздер: *легирленген болат, ішкі үйкеліс, соққы шуы, дірілді сөндіру, микроқұрылым, серпімділік модулі, меншікті электр кедергісі, акустикалық эмиссия.*

Микроструктура, внутреннее трение и акустический отклик при ударном воздействии у новых легированных сталей

Р.Ж. Абуова*, Г.А. Буршукова, Е.С. Меркибаев
Международная образовательная корпорация, Алматы, Казахстан
**Автор для корреспонденции: ryskena@mail.ru*

Аннотация. В данном исследовании оцениваются взаимосвязи между диссипацией механической энергии, упругой жесткостью, электрическим сопротивлением, микроструктурной неоднородностью и звуковым излучением при ударном воздействии для трех новых видов легированной стали (XSM-1, XSM-2 и XSM-3). В качестве эталонных материалов использовались стандартные углеродистые стали марок Ст.10, Ст.20 и Ст.45. Образцы в форме пластин (50×50×5 мм) подвергались испытаниям на удар стальным шариком; при этом регистрировались переходные осциллограммы в окне наблюдения длительностью 2 мс. Дополнительные данные были получены в ходе измерений крутильных колебаний и уровня звука, а также при проведении металлографических исследований. Сталь XSM-1 продемонстрировала наибольшее внутреннее трение (21.22×10^{-4}) и наименьший уровень звука по шкале A (72 дБА), тогда как для эталонных сталей эти показатели составили $9.11\text{-}10.565\times10^{-4}$ и 84-89 дБА соответственно. Для сталей XSM-2 и XSM-3 уровни звука составили 77 дБА и 87 дБА, несмотря на относительно высокое внутреннее трение в обоих случаях. Коэффициент корреляции Пирсона между внутренним трением и уровнем звука для всех шести исследованных материалов составил приблизительно −0.70, в то время как значения модуля упругости не обнаружили четкой монотонной зависимости. Микрофотографии стали XSM-3 указывают на структурную неоднородность, однако не позволяют однозначно идентифицировать фазовый состав. Результаты показывают, что внутреннее демпфирование материала играет важную роль, но его одного недостаточно для прогнозирования шума при ударе; необходимо учитывать совокупность факторов: модальный отклик, микроструктуру и условия проведения испытаний. В рамках данного сравнительного исследования сталь XSM-1 выделена как наиболее перспективный вариант; также определен перечень измерений, необходимых для независимой проверки полученных результатов.

Ключевые слова: *легированная сталь, внутреннее трение, ударный шум, виброгашение, микроструктура, модуль упругости, удельное электрическое сопротивление, акустическая эмиссия.*

Publisher's note

All claims expressed in this manuscript are solely those of the authors and do not necessarily represent those of their affiliated organizations, or those of the publisher, the editors and the reviewers.